water

MDPI

Article

Biodegradation and Decolorization of Textile Azo Dyes by *Paramecium caudatum* Isolated from Industrial Wastewater

Uzma Ramzan [1], Farah Rauf Shakoori [1,*], Muhammad Tariq Zahid [2], Waqar Majeed [3,*], Itrat Zahra [1], Syed Zaghum Abbas [4], Amor Hedfi [5], Sabry Hassan [5], Abdul Rauf Shakoori [6,*] and Abdullah Al Mutery [7,8,*]

1 Institute of Zoology, University of the Punjab, Quaid-i-Azam Campus, Lahore 54590, Pakistan
2 Department of Zoology, Government College University Lahore, Lahore 54000, Pakistan
3 Department of Zoology Wildlife and Fisheries, University of Agriculture, Faisalabad 38000, Pakistan
4 Biofuels Institute, School of Environment and Safety Engineering, Jiangsu University, 301 Xuefu Road, Zhenjiang 212013, China
5 Department of Biology, College of Sciences, Taif University, P.O. Box 11099, Taif 21944, Saudi Arabia
6 School of the Biological Sciences, University of the Punjab, Quaid-i-Azam Campus, Lahore 54590, Pakistan
7 Department of Applied Biology, College of Sciences, University of Sharjah, Sharjah 727272, United Arab Emirates
8 Human Genetics & Stem Cells Research Group, Research Institute of Sciences & Engineering, University of Sharjah, Sharjah 727272, United Arab Emirates
* Correspondence: aalmutery@sharjah.ac.ae (A.A.M.); farah.zool@pu.edu.pk (F.R.S.); waqar.majeed@uaf.edu.pk (W.M.); arshakoori.sbs@pu.edu.pk (A.R.S.)

Abstract: Azo dyes in textile industry effluent are one of the major toxic contaminants causing a severe threat to life. Bioremediation is the most cost-effective and environmentally beneficial innovative biotechnologically technique used to mitigate dyes' toxic effects in aquatic environments. The purpose of the present study was to determine the azo dyes degradation potential of a ciliate, *Paramecium caudatum*, isolated from industrial wastewater. Under optimum conditions, *P. caudatum* was found to possess a 90.86% decolorizing ability of RR2 (reactive red), 83.06% of RB5 (reactive blue) and 85.43% of LY (Levafix reactive yellow) dyes. The *P. caudatum* showed maximum growth at 25 °C and pH 7.5 in the presence of azo dyes at a concentration of 20 ppm (0.02 mg/mL). After being exposed to RR2, RB5, and LY azo dyes, the level of GSH in *P. caudatum* increased for the control i.e., 54, 43, and 23%, respectively. Sequentially, the GSSG level decreased by 26% after treatment with the LY azo dye, while exposure to RR2 and RB5 enhanced the value by more than twofold and by 0.86%. The results for the decolorization and biodegradation of azo dyes indicated that *P. caudatum* is a potential candidate for the treatment of textile industry effluents.

Keywords: azo dyes; biological treatment; detoxification; *Paramecium caudatum*; textile effluents

check for updates

Citation: Ramzan, U.; Shakoori, F.R.; Zahid, M.T.; Majeed, W.; Zahra, I.; Abbas, S.Z.; Hedfi, A.; Hassan, S.; Shakoori, A.R.; Mutery, A.A. Biodegradation and Decolorization of Textile Azo Dyes by *Paramecium caudatum* Isolated from Industrial Wastewater. *Water* **2022**, *14*, 3553. https://doi.org/10.3390/w14213553

Academic Editors: Xuwang Zhang and Yuanyuan Qu

Received: 9 October 2022
Accepted: 31 October 2022
Published: 4 November 2022

Publisher's Note: MDPI stays neutral with regard to jurisdictional claims in published maps and institutional affiliations.

1. Introduction

A major source of environmental pollution is azo dyes. Due to their widespread usage in various industries, particularly in the textile, plastic, pharmaceutical, cosmetics, food, leather and printing industries [1–3], and a substantial part (17–20%) of textile-based industrial waste comprises dye effluents [4,5]. About 200,000 dye stuffs [6], of which 30,000 tons of azo dyes, are discharged into aquatic ecosystems each year [7]. This also results in air and soil contamination, which significantly deteriorates the quality of life when an industry is not well equipped to treat its waste properly before throwing it into aquatic environments. Dyes at a commercial level are categorized as anthraquinone, basic, acidic, dispersal, and azo dyes. Azo dyes have an azo group (−N = N−) in their structure and contain naphthalene and benzene rings [8]. In addition to them, 80% are present in the azo group [9]. Azo dyes molecules are poisonous, carcinogenic, teratogenic and mutagenic, making them detrimental to higher living species including aquatic ecosystems and plants [10,11].

Approximately 15–20% of azo dyes are not fixed to the substrate and are released as wastewater into aquatic environments. The existence of minute amounts of azo dyes is extremely noticeable and has a severe impact on the clarity and quality of water bodies such as lakes, ponds and rivers, posing a severe danger to aquatic fauna and indirectly to human health [12]. The coloration of the dyestuff disrupts the aquatic ecosystem by decreasing sunlight penetration, resulting in eutrophication, ultimately reducing the photosynthetic activity of plants, affecting the food chain and halting water reoxygenation [13,14]. The solubility of gas, changes in pH and increases in the BOD, TOD and COD of water properties present detrimental consequences [15].

Treatment methods for wastewater that is spoiled because of azo dyes are generally classified in three types, i.e., chemical, physical and biological [16]. The physical or chemical treatment approaches are filtration, flocculation, adsorption, coagulation, electrochemical oxidation, Fenton reaction and oxidation processes. All the above-mentioned methods are inefficient due to various limitations, including being expensive and time-consuming, producing a huge amount of waste that is extremely toxic and complicated to throw away safely [17]. Different pathways and mechanisms have been used for the degradation of azo dyes by microorganisms [18,19]. In anaerobic conditions, microorganisms degrade azo dyes by using azo-reductase enzymes and convert it into colorless aromatic amines [20,21]. The microbial strains have the ability to degrade and transform many toxic compounds into non-toxic end products [22]. The cleavage of the chromophore groups of azo dyes results in the colorless, odorless and toxic intermediate metabolites of aromatic amines, which are commonly mineralized under aerobic conditions [23]. The resulting intermediate metabolites are further degraded aerobically or anaerobically [24,25].

Bioremediation is regarded as an ecologically friendly technique used to degrade azo dyes, and its efficacy is dependent upon the activity and adaptation of microorganisms [26]. Bacteria degrade azo dyes and produce more resistant and hazardous aromatic amine compounds, prohibiting the widespread use of clean the azo-dye-containing industrial effluents [27]. The elimination of dyes by using fungus is also restricted in textile wastewater treatment plants because of bacterial contamination and unsafe management. Moreover, other microorganisms such as protozoa, which are natural microflora in water bodies, can enhance their effectiveness [28].

Protozoa play a significant role in biological wastewater treatment systems. These organisms dominate in terms of biomass and numbers and alter the mineralization and elimination process of inorganic and organic nutrients [29]. These are single-cell microorganisms that lack a protective cell wall, allowing them to respond directly to environmental stimuli. Ciliates, particularly *Paramecium*, due to their short life cycle, high rate of reproduction, cosmopolitan distribution, high diversity and quick response to environmental changes make them perfect biological indicators for aquatic ecosystem risk evaluation [30]. The present research work aimed to characterize the *Paramecium* sp. and to determine its azo-dyes-degradation ability and optimum growth conditions for the efficient degradation and decolorization of azo dyes in textile-based industrial wastewater.

2. Materials and Methods

2.1. Dyes Used

The azo dyes, Reactive Red 2 (RR2), Reactive Blue 5 (RB5) and Levafix Yellow Reactive (LY) used in current study were purchased from Sigma-Aldrich. Stock solutions (0.1%) of these dyes prepared in distilled water were further diluted to 20 ppm (0.02 mg/mL) for use in the experiments.

2.2. Isolation, Purification and Maintenance of Paramecium sp.

Paramecium sp. was isolated by the drop method and inoculated in Bold basal salt medium (BBSM) from textile industry effluents containing algae, fungi and bacteria. To remove the algae, the culture was placed in the dark. To remove the fungi and bacteria, antibiotics, i.e., amphotericin B (1 ug/mL) and kanamycin (50 ug/mL) were used,

respectively. The pure culture of *Paramecium* was maintained according to Shakoori and Rehma [31]. Bold basal salt medium [$NaNo_3$ 0.25 g/L, NaCl 0.0025 g/L, $MnCl_2.4H_2O$ 0.00144 g/L, $CaCl_2.H_2O$ 0.025 g/L, $ZnSO_4.7H_2O$ 0.00881 g/L, K_2HPO_4 0.075 g/L, H_3BO_3 0.01142 g/L, $CuSO_4.5H_2O$ 0.00157 g/L, EDTA 0.05g/L, H_2SO_4 0.001 L/L, $FeSO_4.7H_2O$, MoO_3 0.00071 g/L, KOH 0.031 g/L, $MgSO_4.7H_2O$ 0.075 g/L, KH_2PO_4 0.175 g/L and $Co(NO_3).6H_2O$ 0.00049 g/L] was used, and 4–6 wheat grains in 30 mL of distilled water were inoculated with a water sample containing *Paramecium* sp.

2.3. Molecular Characterization of Paramecium sp.

Genomic DNA of ciliate at the log phase was separated by the phenol–chloroform extraction method of Sambrook et al. [32]. The 18S rRNA gene was amplified using 18S universal primers, i.e., Euk-F (5′-AATATGGTTGATCCTGCCAGT-3′) and Euk-R (5′-TGATCCTCCTGCAGGTTCACCTAC-3′). The thermal cycle comprised an initial denaturation at 94 °C for 5 min followed by 35 cycles, each denaturation being at 94 °C for 1 min, annealing at 55 °C for 2 min and extension at 72 °C for 2 min. The final extension was conducted at 72 °C for 10 min [33]. The PCR product (1.8k bp) was purified using a gel extraction kit and was sequenced at Macrogen (South Korea). The sequence was analyzed by NCBI using the Basic Alignment Search Tool (BLAST) and snapGene software and submitted to Genbank [34].

2.4. Decolorization at Different Temperatures and pH

To determine the optimum conditions (temperature and pH) for the decolorization of azo dyes, the axenic culture of *Paramecium* at the log phase was inoculated with azo dyes (RR2, RB5 and LY) at a concentration of 20 ppm. The effect of the temperature was analyzed by incubating at 20, 25, 30 and 35 °C. The medium was maintained at different pH values (i.e., 6, 7, 7.5 and 8). The decolorization of azo dyes was observed after every 24 h for 10 days by using a UV-Spectrophotometer. Graphs of the decolorization of the dyes at different temperatures and pH values were plotted.

2.5. Decolorization Potential of Paramecium sp.

Decolorizing of RR2, RB5 and LY azo dyes using the *Paramecium* sp. strain was conducted in a 500 mL conical flask comprising 100 mL *Paramecium* pure culture. When the culture was in the log phase, these azo dyes were added from the stock solution to make a final concentration 20 ppm. After every 24 h, 1.5 mL of sample was taken in a microfuge tube and centrifuged at 12,000 rpm for 30 min. The optical density of the clear supernatant was measured at 550 nm by using a UV–visible spectrophotometer. The whole experiment, including the control, was performed in triplicate for 10 days until the decolorization of azo dye was complete. The percentage decolorization was calculated by using the following given formula [35].

$$\text{Decolorization } (\%) = \frac{\text{Initial absorbance} - \text{Final absorbance}}{\text{Initial absorbance}} \times 100$$

2.6. Growth of Paramecium sp. at Different Temperatures and pH values in the Lag Phase

To determine the optimum temperature in the lag phase, the experiment was set in triplicate. For this, 500 µL of pure culture of *Paramecium* was inoculated in 30 mL BBSM in thirty-six (250 mL) conical flasks containing a 20 ppm (0.02 mg/mL) concentration of each azo dye RR2, RB5, and LY, respectively, and for the control experiment, twelve flasks were also inoculated with the pure culture. All the flasks were placed at different temperatures (i.e., 20 °C, 25 °C, 30° C and 35 °C). Cells were counted after every 24 h for 12 days. Graphs for each temperature were plotted.

To determine the optimum pH for the growth of *Paramecium* in the lag phase, flasks were prepared according to the above-mentioned method and maintained at pH values of 6, 7, 7.5 and 8. Cells were counted under a light microscope after every 24 h for 12 days. Graphs for each pH value were plotted.

2.7. Analysis of Dye Degraded Products

Fourier transform infrared spectroscopy (FTIR) was performed to characterize biodegradation products. The variation in the functional group of the azo dyes before and after treatment with UR03 strain was analyzed. Treated samples were centrifuged at 14,000 rpm for 30 min. A carry 360 spectrophotometer was used to record FTIR spectra in the 650–4000 cm^{-1} infrared region [36]. Results were interpreted by using origin pro 9.1 software.

The total protein of the dye-treated and control *Paramecium* samples were quantified according to the Bradford [37] method by taking the OD at 595 nm against blanks via a UV spectrophotometer. The treated samples were exposed to azo dye for 96 h.

2.8. Estimation of Glutathione Contents

The rate of reduced (GSH), oxidized (GSSG) and total glutathione (GSH+GSSG) of the control and azo-dyes-treated *Paramecium* cultures were quantified according to the method of Israr et al. [38].

2.9. Statistical Analysis

Values in tables and figures were observed as the mean and standard error (SE) of the mean. The experiment was conducted with three replicates for each factor. Statistical analysis was accomplished by using one-way ANOVA followed by the Dunnett test. Significant differences in each treatment relative to the control were analyzed in Minitab 17 software.

3. Results

3.1. Paramecium Caudatum (UR03) as Efficient Dye Decolorizer

Among the five different isolates (UR01, UR02, UR03, UR04 and UR05), UR03, identified as *Paramecium caudatum*, had the maximum ability to decolorize the azo dyes. For the molecular identification, the 18S rRNA gene PCR product was sequenced, and the sequence was submitted to the Genbank database under the accession number MZ540257. The PCR product of the 18S rRNA gene in 1% agarose gel is represented in Figure 1. The phylogenetic tree of *P. caudatum* with other species of same genus is shown in Figure 2. The phylogenetic tree represented that *P. caudatum* was the most homogenous to *P. schewiakoffi* (LT628501.1), and *Paramecium duboscqui* was taken as the outgroup. The BLAST analysis of the molecular sequences of 18S rRNA showed that UR03 was a ciliate, showing 99.11% homology with those of other ciliates.

Figure 3 shows the efficiency of the degradation of the azo dyes by *Paramecium caudatum* at different temperatures and pH values. It was observed from the experiment that *P. caudatum* showed the maximum decolorization ability at a temperature of 25 °C (Figure 3a) and pH 7.5 (Figure 3b), which is the normal temperature and pH for its maximum growth.

3.2. Decolorization of RR2, BB5 and LY

Figure 4 shows the decolorizing ability of UR03 strain. *P. caudatum* showed a maximum of 90.86, 83.06 and 85.43% decolorization of RR2, RB5 and LY, respectively (Table 1). After 240 h (10 days) time interval expressed in Figure 4a and decolorization of dyes were observed, as shown in Figure 4b.

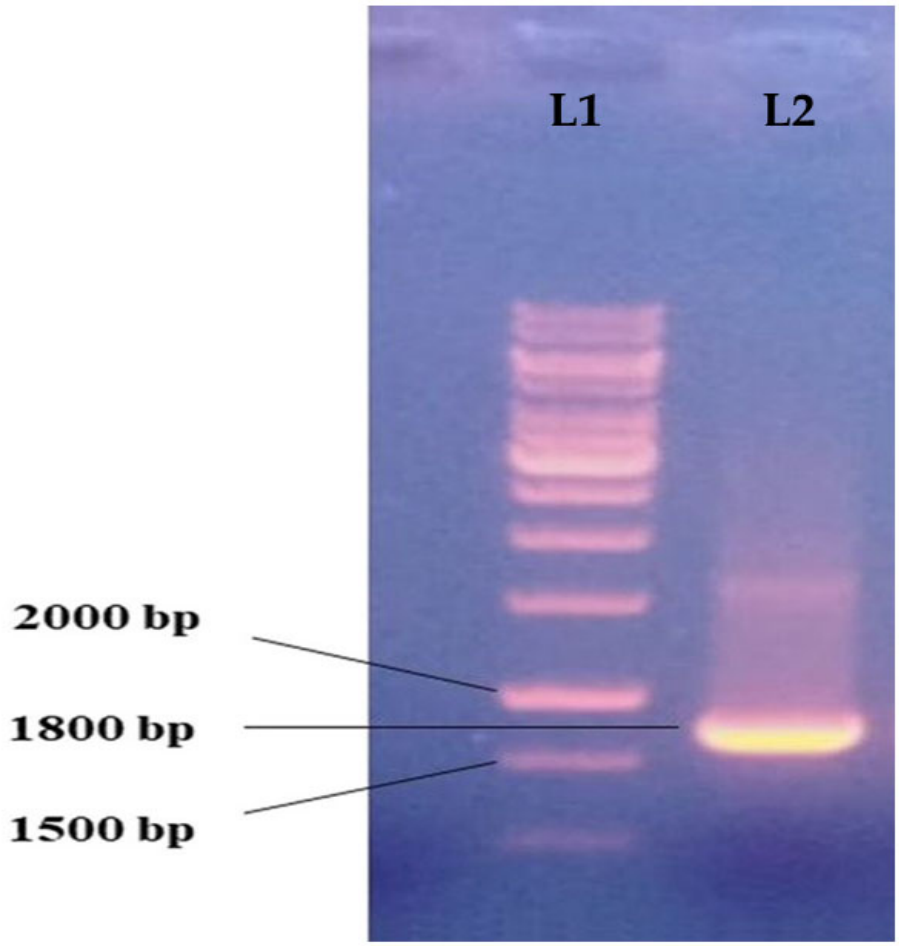

Figure 1. Lane 1, 1kb molecular weight marker; lane 2, PCR amplification of 18S rRNA gene of ciliate UR03 isolated from industrial wastewater.

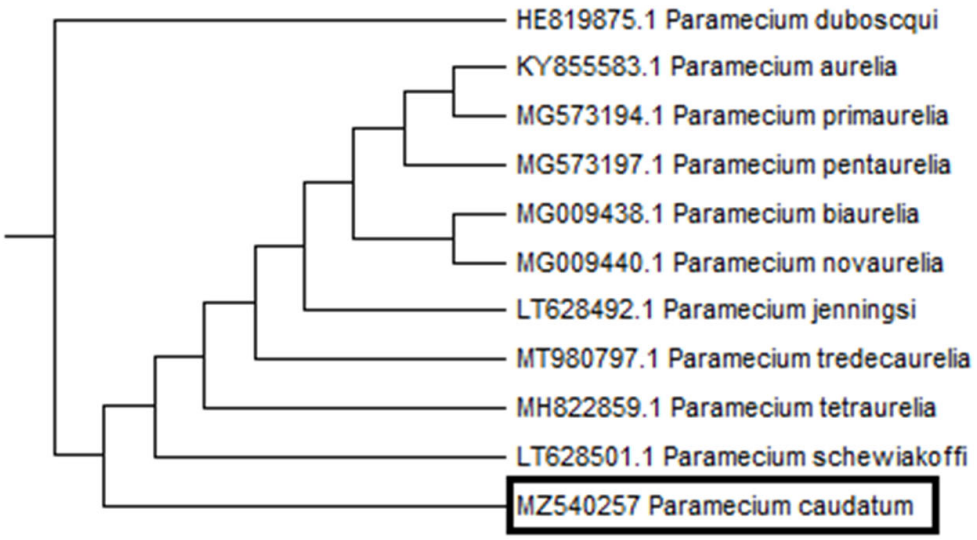

Figure 2. Phylogenetic tree of *Paramecium caudatum* with other species of genus *Paramecium*. The corresponding nearest sequencing was retrieved from NCBI database and tree was constructed by using Tree View X software. *Paramecium duboscqui* was taken as outgroup.

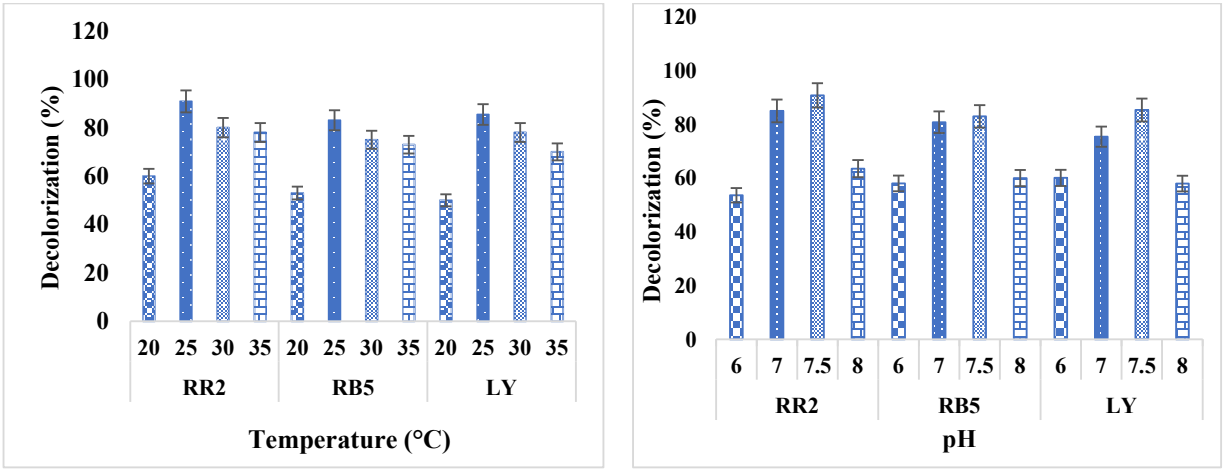

Figure 3. Decolorization of azo dyes by *Paramecium caudatum* UR03, (**a**) at different temperatures (20, 25, 30 and 35 °C) and (**b**) different pH (6, 7, 7.5 and 8).

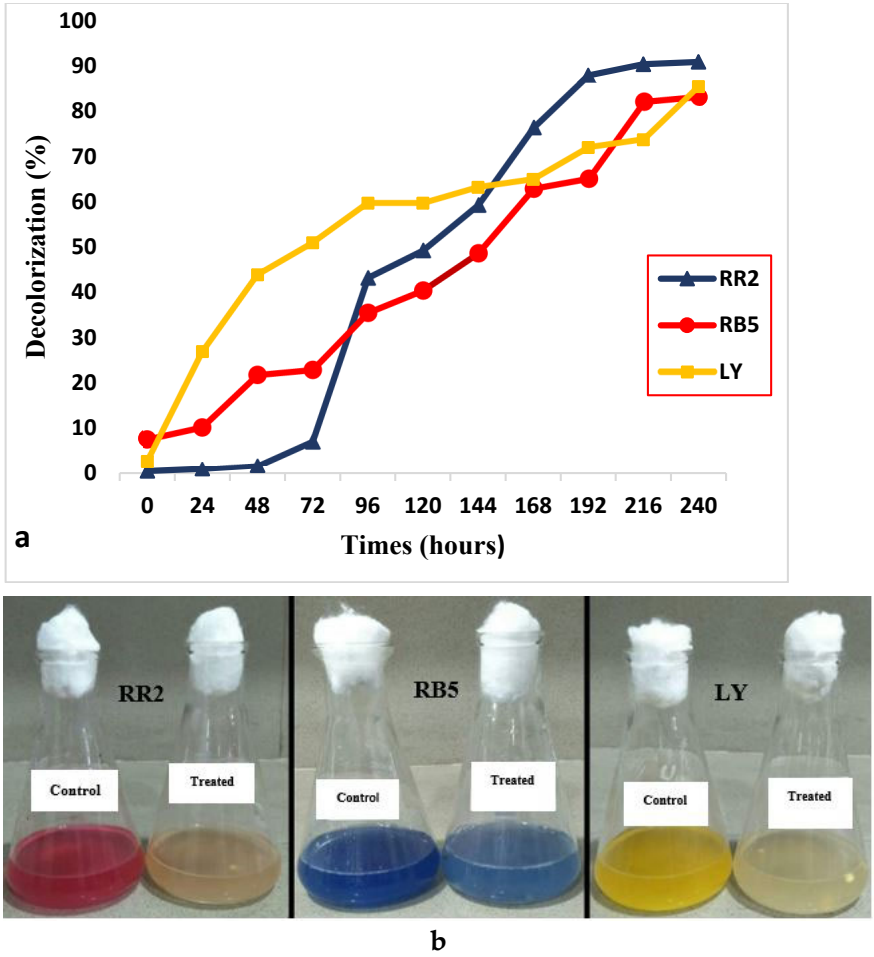

Figure 4. Decolorization/degradation of different dyes by *P. caudatum* UR03 in 100 mL of culture medium inoculated with 10 ul of azo dyes over a period of 10 days. (**a**) Showed the decolorization profile of different dyes monitored after every 24 h for 10 days. (**b**) Showed the azo dye degradation as indicated by decolorization in the flasks.

Table 1. Azo dyes degradation ability of *Paramecium* isolates. Percent decolorization is indicative of degradation ability.

Isolate	RR2 (%)	RB5 (%)	LY (%)
UR01	70.88	70.00	63.55
UR02	80.00	75.02	70.00
UR03	90.86	83.06	85.43
UR04	80.00	60.08	74.00
UR05	40.22	51.00	50.00

3.3. Optimum Temperature and pH for Maximum Growth

Paramecium caudatum showed the maximum growth (4×10^3 cells/mL) at 25 °C in the RR2 azo dye, whereas RB5 and LY exhibited the highest growth of 5×10^3 and 2.6×10^3 cell/mL, respectively, at this temperature (Figure 5). At the optimum pH (7–7.5), a maximal growth rate was noted. At pH 7.5, *P. caudatum* treated with RR2 azo dye depicted the highest growth of 4×10^3 cells/mL. However, significant growth was recorded for RB5 and LY, i.e., 4.4×10^3 and 4.8×10^3 cells/mL, respectively (Figure 6).

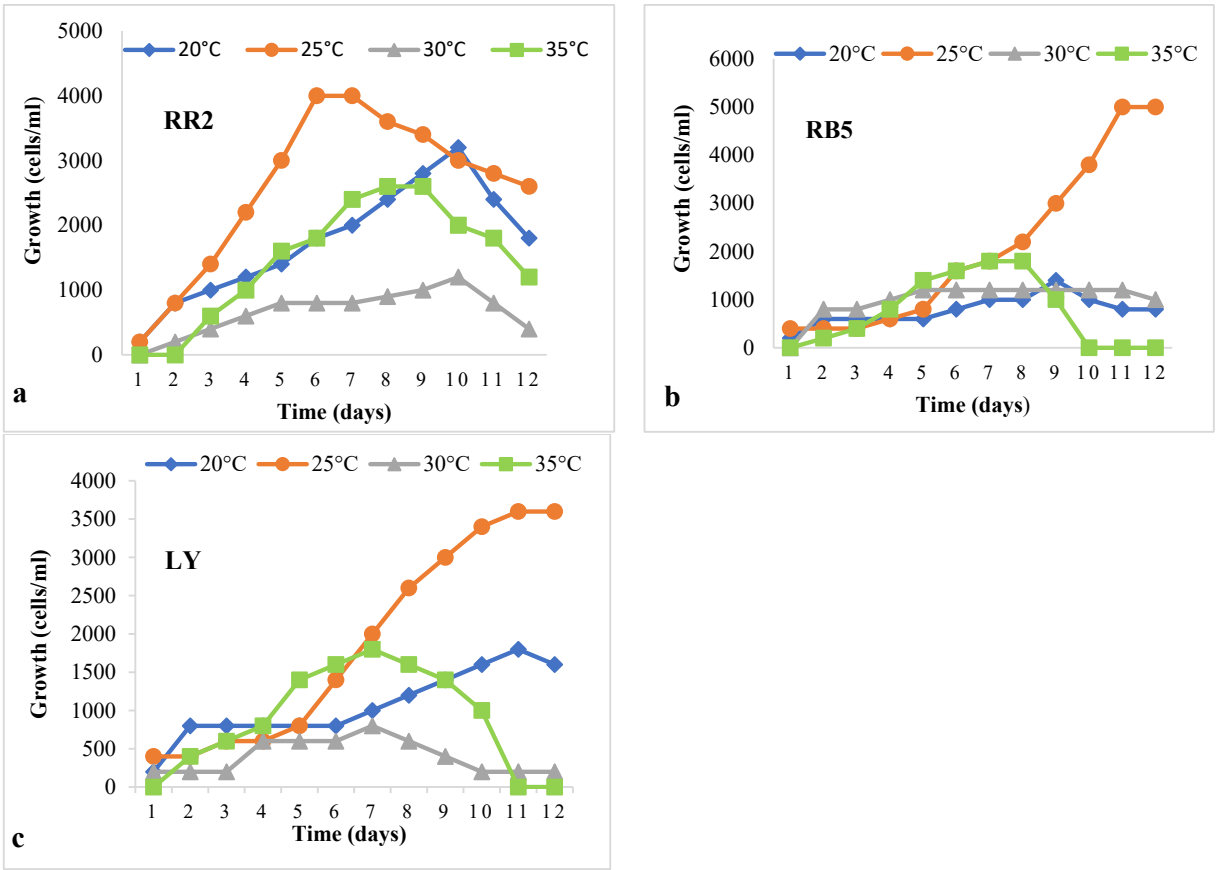

Figure 5. Growth curves of *P. caudatum* UR03 in culture medium containing azo dyes, RR2 (**a**), RB5 (**b**) and LY (**c**) at different temperatures.

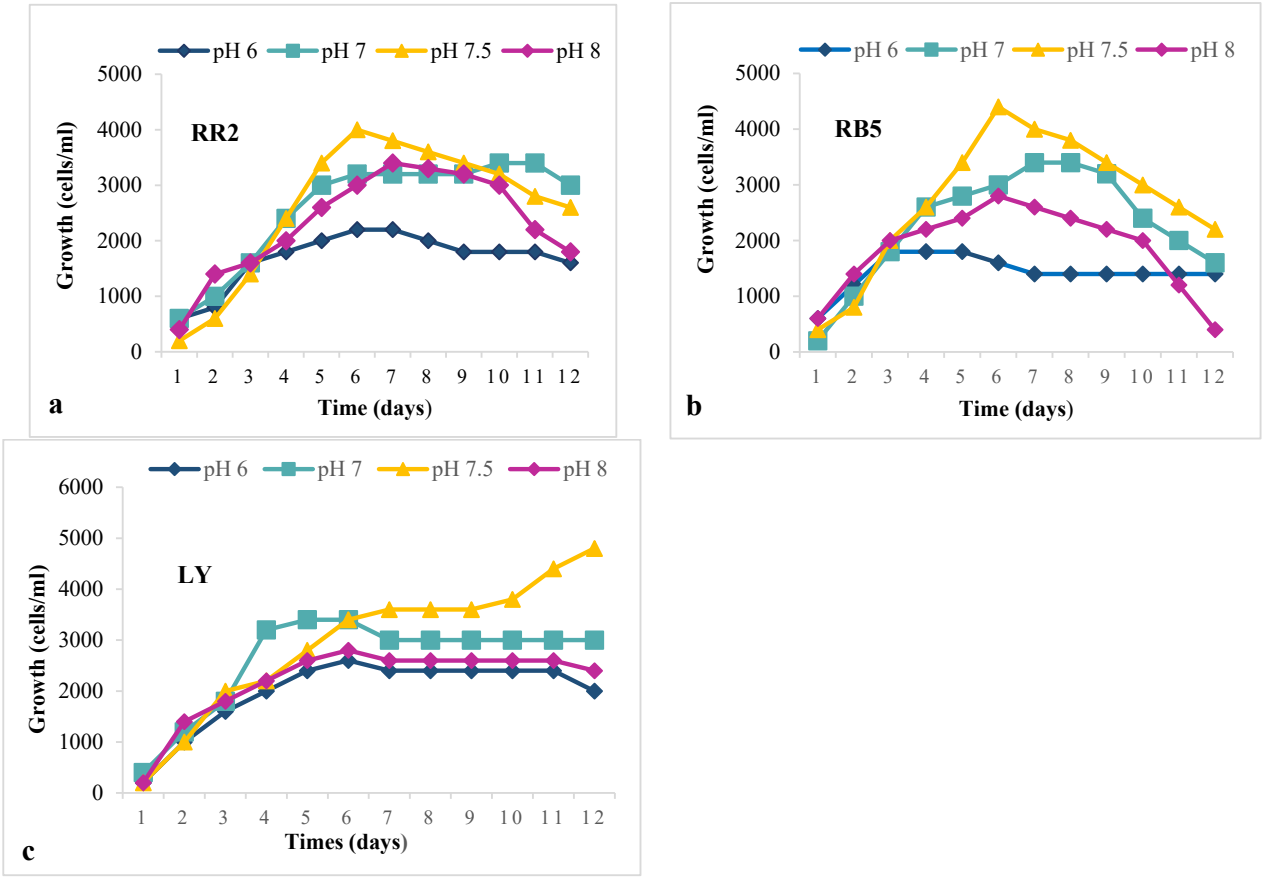

Figure 6. Growth curve of *P. caudatum* UR03 in culture medium containing azo dyes, RR2 (**a**), RB5 (**b**) and LY (**c**) at different pH values.

3.4. Degradation Products of Azo Dyes

Azo dye molecules as a powder were analyzed by FTIR in the control and treated samples (Figure 7). The FT-IR spectra of the control of RR2 dye (Figure 7a) displayed the following absorbance of bands: 3411 cm^{-1} (-NH_2), 2100 cm^{-1} (Si-H silane), 1632 cm^{-1} (-N=N-), 1530 cm^{-1} (N=O), 1448 cm^{-1} (C-H), 1380 cm^{-1} (O-H), 1115 cm^{-1} ($SO_3{}^{-2}$), 1034 cm^{-1} (S=O), 743 cm^{-1} (S-OR) and 600 cm^{-1} (C-Cl) as compared to the spectra of the treated sample, with RR2 azo dye (Figure 7b) bands appearing at 3431 cm^{-1} (OH), 1618 cm^{-1} (N=N), 1490 cm^{-1} (C=N) and 1054 cm^{-1} (C-O).

However, the FTIR spectra of the RB5 control dye (Figure 7c) showed the following bands: 3465 cm^{-1} (-NH_2), 1584 cm^{-1} (-N=N-), 1489 cm^{-1} (C=C), 1211 cm^{-1} (C-C), 1115 cm^{-1} ($SO_3{}^{-1}$), 1041 cm^{-1} (C-O), 986 cm^{-1} (C = H), 892 cm^{-1} (C-Cl), 831 cm^{-1} (S-OR), 730 cm^{-1} (-C=O) and 613 cm^{-1} (C-Br), compared with the spectra of the treated RB5 dye (Figure 7d) representing bands at 3247 cm^{-1} (N-H), 2093 cm^{-1} (C-C) and 1638 cm^{-1} (C=N).

However, the FTIR spectra for the LY control dye (Figure 7e) showed bands at 3441 cm^{-1} (N-H), 1614 cm^{-1} (C=C), 1482 cm^{-1} (C=C), 1110 cm^{-1} (P=O), 1006 cm^{-1} (S=O) and 737 cm^{-1} (-NO_2), compared with the spectra of the treated LY dye (Figure 7f) showing bands at different wavelengths, i.e., 3400 cm^{-1} (N-H), 1544 cm^{-1} (N=O), 1394 cm^{-1} (CH_3) and 1129 cm^{-1} (P=O). The disappearance of the spectra in the treated samples was due to the complete breakdown of the dye molecule and the corresponding shift in functional group peaks compared to the control.

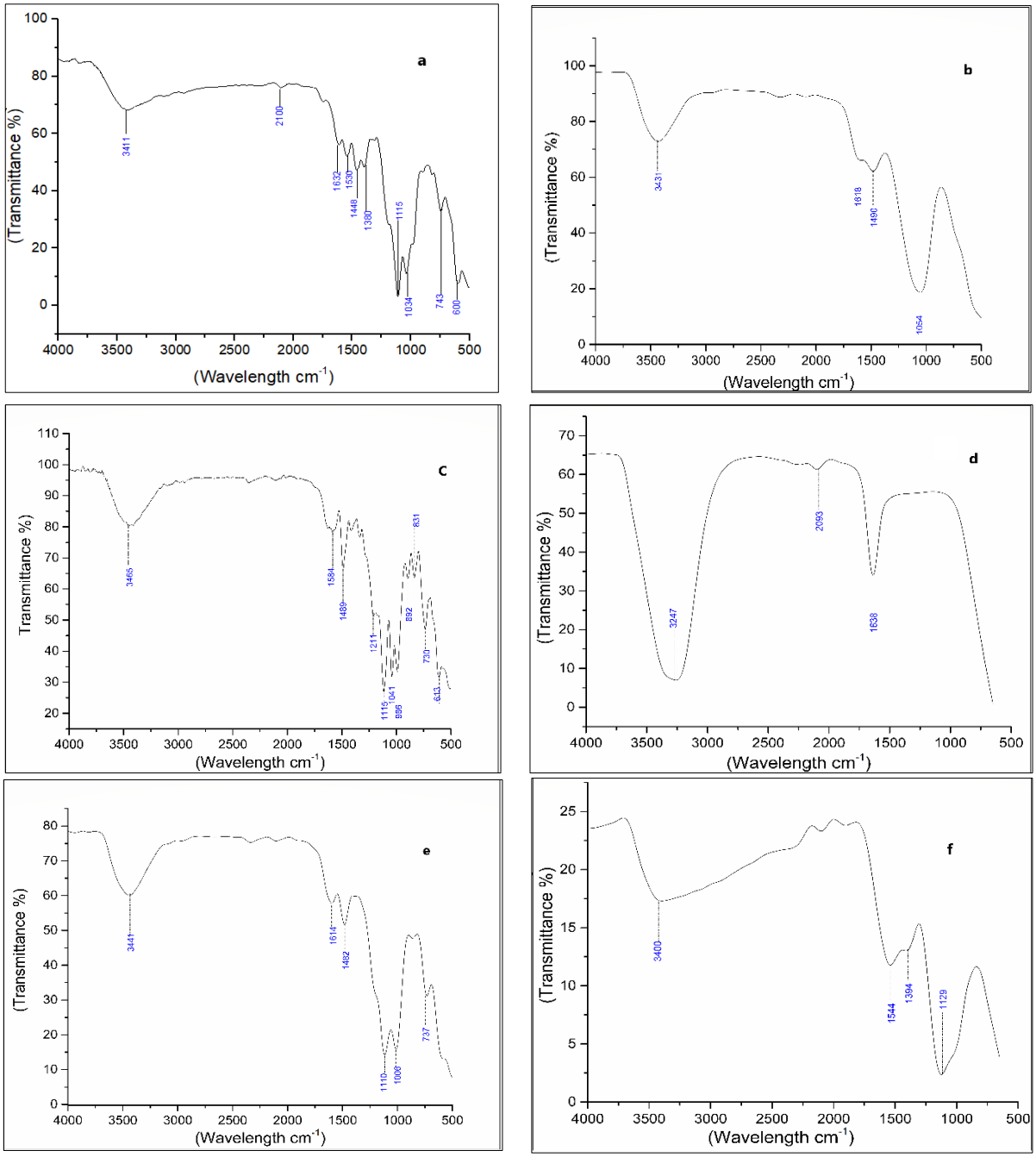

Figure 7. FTIR spectra of (**a**) RR2 control dye, (**b**) RR2 treated dye, (**c**) RB5 control dye, (**d**) RB5 treated dye, (**e**) LY control dye and (**f**) LY treated dye.

3.5. Total Protein Contents

P. caudatum showed a significant ($p < 0.000$) rise in protein content after treatment with RR2, RB5 and LY azo dyes (81%, 139% and 42%, respectively) (Table 2).

Table 2. Effect of different azo dyes on the total protein content of *P. caudatum* (UR03).

Variable	Total Protein Content (ug/mL)
Control	25.363 ± 0.27 a
RR2	45.790 ± 0.15
RB5	60.837 ± 0.56
LY	36.073 ± 0.21

Note(s): Mean not labeled with letter a are significantly different from control level mean.

3.6. Glutathione Contents

The treatment of azo dyes altered the level of GSH and GSSG in *P. caudatum*. After being exposed to the RR2, RB5 and LY azo dyes, the level of GSH in *P. caudatum* increased for the control, i.e., 54, 43 and 23%, respectively. Sequentially, the GSSG level decreased by 26% after treatment with the LY azo dye, while exposure to RR2 and RB5 enhanced the value by more than twofold and by 0.86%. Similarly, the GSH/GSSG ratio also increased after exposure to the azo dyes (Table 3).

Table 3. Effect of different dyes administered at a concentration of 20 ppm on the glutathione level in *P. caudatum* UR03.

Groups	GSH (mM g^{-1})	GSSG (mM g^{-1})	GSH + GSSG (mM g^{-1})	GSH/GSSG Ratio
Control	2.898 ± 0.04 a	0.764 ± 0.04 a	3.662 ± 0.01 a	3.818 ± 0.25 a
RR2	4.463 ± 0.04	2.737 ± 0.02	7.200 ± 0.02	1.631 ± 0.03
RB5	4.155 ± 0.02	1.421 ± 0.03	5.576 ± 0.01	2.926 ± 0.08
LY	3.575 ± 0.02	0.562 ± 0.02	4.136 ± 0.01	6.377 ± 0.21

Note(s): Mean not labeled with letter a are significantly different from control level mean. GSH, reduced glutathione; GSSG, oxidized glutathione.

4. Discussion

The textile industries are considered one of the world's main environmental contamination issues since they produce unwanted coloring effluents [39]. Wastewater has to be treated appropriately before being released into aquatic ecosystems. Residual dyes contain structurally complex compositions that are harmful to aquatic life. Dyes cannot be fully degraded by physicochemical processes such as adsorption, oxidation, coagulation, electrochemical methods and flocculation [40]. Microbial and enzymatic wastewater decomposition is a feasible alternative since it does not create significant sludge quantities, is cheap and has no detrimental environmental impact [41].

In the current research, we studied the use of *Paramecium* sp. as a model organism, which was used to decolorize azo dyes in textile sewage. The most frequently utilized ciliates are freshwater protozoans such as Paramecia, which are considered good bioindicators for toxicity stress and chemical pollution [42]. Considering the significance of these organisms, *Paramecium* species have been identified from samples of azo-dye-polluted textile industrial wastewater. Furthermore, the morphology and ribotyping were confirmed as *Paramecium caudatum*. *Oxytricha fallax* and *P. caudatum* have been recognized as a potential bio-remediator of polluted wastewater, as these different ciliates have been isolated from wastewater that is resistant to any heavy metals [43].

The isolated *Paramecium* sp. had a high ability to decolorize the azo dyes. The decolorization potential of *Paramecium caudatum* was 90.87%, 83.06% and 85.43% against RR2, RB5 and LY azo dyes, respectively. This study was the first time that azo dyes have been reported to be degraded by *Paramecium* sp. According to Ponraj et al. [44], bacteria (*Bacillus* sp.) has a powerful degradation and decolorization capability for the azo dye Orange 3RS. The isolation of *Pseudomonas* sp., *Klebsiella* and *Salmonella* was conducted from wastewater from the textile industry, and under optimal conditions the decolorization of Orange 3RS was analyzed, which represented that *Pseudomonas* sp. and *Bacillus* sp. depicted a parallel level of decolorization (92%), followed by *Salmonella* sp. (80%) and *Klebsiella* sp. (76%). Sulfate-reducing bacteria can decolorize RR2 up to 78% [45].

The pH effect was observed at different pH values (i.e., 6, 7, 7.5 and 8). Growth was observed at all pH values, but the maximum growth of *P. caudatum* and the maximum decolorization of the azo dyes was shown at pH 7.5 after exposure to azo dyes, and the temperature for the highest growth was at 25 °C after exposure to azo dyes. The pH level of 6.0 and above 8.0 was not suitable for ciliates *T. farahensis,* while these organisms could be optimally grown in the pH range of 7.0–7.5 [46]. The tolerance of pH for coloring microbes is essential since dyes are attached under basic conditions and elevated temperatures to cotton fibers by additional or replacement processes. Many other scientists have also used this optimal temperature (27 ± 1 °C) to culture other species of *Tetrahymena* [47].

The FTIR of the generated periphyton metabolism revealed significant changes, as particular peaks in the control sample disappeared and new peaks were developed. The disappearance of peaks related to the azo group was due to the breakdown of the azo bond. The disappearance of many peaks occurred in the RR2-dye-treated samples, including Si-H silane at 2100 cm^{-1}, N=O at 1530 cm^{-1}, S-OR at 743 cm^{-1} and C-Cl stretching at 600 cm^{-1}, while in the RB5-exposed samples, the removal of -N=N- at 1584 cm^{-1}, C-C (aromatic ring) at 1211 cm^{-1}, C-O at 1041 cm^{-1} and Alkyl halide (C-Br) at 613 cm^{-1} occurred. In the LY-dye-treated samples, the FTIR spectra lost the peaks related to C=C at 1614 cm^{-1}, S=O at 1006 cm^{-1} and NO_2 at 737 cm^{-1}. Khan et al. [48] proposed that the absence of functional groups in dye-treated samples was cleaved to adjacent compounds. The azo bond decolorization of the control group showed a different wavelength spectrum in the FTIR compared with the sample of the *Marinobacter* sp. strain HBRA exposed to Reactive Blue 1 dye [3].

The current research estimated that the total protein content increased after being treated with azo dyes. This result was comparable with the outcomes of Amamra et al. [49], who observed an increase in the total protein rates in a dose-dependent approach when studying the impact of an insecticide, cypermethrin, on the ciliate *Paramecium tetraurelia*. The presence of xenobiotics in the cell promotes the protein synthesis of several enzymes and corresponds to their capacity to metabolize and detoxify harmful substances. This trend may be due to a higher protein rate [50]. Through a redox and detoxifying process, GSH maintains the normal structure and function of the cells [51]. In this study, the level of GSH increased in *Paramecium* sp. after treatment with the azo dyes. The GSH level of the *Paramecium* species increased when it was treated with higher concentrations of Chlorfenapyr. As a reductant and antioxidant, a high-level ratio of GSH/GSSG was required to maintain glutathione's function [52]. This ratio fluctuated according to the physiological condition of the cells, such as proliferation, differentiation or death, and its disruption had a substantial impact on the signaling processes of the cells. The regulatory influence that GSH/GSSG has on the functional activity of proteins was primarily responsible for this role. A significant increase in glutathione content was observed, which indicated the oxidative stress caused by azo dyes [53–55].

5. Conclusions

Textile industry effluent containing hazardous azo dyes is a major obstacle to long-term environmental sustainability. This study was the first report indicating that isolated *Paramecium* sp. (UR03) had promising potential for degrading and decolorizing the three azo dyes used in this study. The *Paramecium* sp. showed the maximum growth at pH 7.5 and temperature 25 °C. The biodegraded products were confirmed with FTIR. Further study should aim to identify the genes present in the *Paramecium* strain that would help to enhance the decolorization and biodegradation of azo dyes.

Author Contributions: U.R., A.R.S. and F.R.S. conceptualized and designed the study. U.R., W.M., M.T.Z., S.Z.A., A.H., S.H., A.A.M., I.Z. and F.R.S. wrote the manuscript. U.R. and W.M. analyzed the data statistically. A.R.S., F.R.S., S.Z.A., W.M., A.H., S.H., A.A.M. and M.T.Z. reviewed the article. A.R.S., U.R., A.H., S.H., W.M., S.Z.A., A.A.M., I.Z. and F.R.S. edited the final manuscript. All authors have read and agreed to the published version of the manuscript.

Funding: This research publication was funded by Taif University with grant number [TURSP-2020/142].

Data Availability Statement: Not applicable.

Acknowledgments: We acknowledge the institute of Zoology (Molecular Biology lab) for providing the facilities to conduct this research work. The authors extend their appreciation to the deanship of scientific research for funding this article by Taif University Research Supporting Project number (TURSP-2020/142), Taif University, Taif, Saudi Arabia.

Conflicts of Interest: All authors declare no conflict of interests among each other.

References

1. Ramzan, U.; Shakoori, F.R.; Shakoori, A.R.; Abbas, S.Z.; Wabaidur, S.M.; Eldesoky, G.E.; Islam, M.A.; Rafatullah, M. Biodegradation and decolorization of Reactive Red 2 azo dye by *Paramecium jenningsi* and *Paramecium multimicronucleatum* in industrial wastewater. *Biomass Convers. Biorefinery* **2022**, 1–9. [CrossRef]
2. Mustafa, G.; Zahid, M.T.; Ali, S.; Abbas, S.Z.; Rafatullah, M. Biodegradation and discoloration of disperse blue-284 textile dye by *Klebsiella pneumoniae* GM-04 bacterial isolate. *J. King Saud Univ.* **2021**, *33*, 101442. [CrossRef]
3. Prasad, A.S.A.; Satyanarayana, V.S.V.; Rao, K.V.B. Biotransformation of Direct Blue 1 by a moderately halophilic bacterium *Marinobacter* sp. strain HBRA and toxicity assessment of degraded metabolites. *J. Hazard. Mater.* **2013**, *262*, 674–684. [CrossRef] [PubMed]
4. Adane, T.; Adugna, A.T.; Alemayehu, E. Textile Industry Effluent Treatment Techniques. *J. Chem.* **2021**, *2021*, 5314404. [CrossRef]
5. Rafiq, A.; Ikram, M.; Ali, S.; Niaz, F.; Khan, M.; Khan, Q.; Maqbool, M. Photocatalytic degradation of dyes using semiconductor photocatalysts to clean industrial water pollution. *J. Ind. Eng. Chem.* **2021**, *97*, 111–128. [CrossRef]
6. Mani, A.; Hameed, S.A.S. Improved bacterial-fungal consortium as an alternative approach for enhanced decolourisation and degradation of azo dyes: A review. *Nat. Environ. Pollut. Technol.* **2019**, *18*, 49–64.
7. Anjaneya, O.; Shrishailnath, S.S.; Guruprasad, K.; Nayak, A.S.; Mashetty, S.B.; Karegoudar, T.B. Decolourization of Amaranth dye by bacterial biofilm in batch and continuous packed bed bioreactor. *Int. Biodeterior. Biodegrad.* **2013**, *79*, 64–72. [CrossRef]
8. Mnif, I.; Maktouf, S.; Fendri, R.; Kriaa, M.; Ellouze, S.; Ghribi, D. Improvement of methyl orange dye biotreatment by a novel isolated strain, *Aeromonas veronii* GRI, by SPB1 biosurfactant addition. *Environ. Sci. Pollut. Res.* **2016**, *23*, 1742–1754. [CrossRef]
9. Balapure, K.; Bhatt, N.; Madamwar, D. Mineralization of reactive azo dyes present in simulated textile waste water using down flow microaerophilic fixed film bioreactor. *Bioresour. Technol.* **2015**, *175*, 1–7. [CrossRef]
10. Chen, B.-Y.; Lin, K.-W.; Wang, Y.-M.; Yen, C.-Y. Revealing interactive toxicity of aromatic amines to azo dye decolorizer *Aeromonas hydrophila*. *J. Hazard. Mater.* **2009**, *166*, 187–194. [CrossRef]
11. Manatunga, D.C.; de Silva, R.M.; Nalin de Silva, K.M.; de Silva, N.; Premalal, E.V.A. Metal and polymer-mediated synthesis of porous crystalline hydroxyapatite nanocomposites for environmental remediation. *R. Soc. Open Sci.* **2018**, *5*, 171557. [CrossRef]
12. Soni, P.; Sharma, S.; Sharma, S.; Kumar, S.; Sharma, K.P. A comparative study on the toxic effects of textile dye wastewaters(untreated and treated) on mortality and RBC of a freshwater fish *Gambusia affinis*(Baird and Gerard). *J. Environ. Biol.* **2006**, *27*, 623–628.
13. Zaharia, C.; Suteu, D.; Muresan, A.; Muresan, R.; Popescu, A. Textile wastewater treatment by homogenous oxidation with hydrogen peroxide. *Environ. Eng. Manag. J.* **2009**, *8*, 1359–1369. [CrossRef]
14. Deniz, F. Color removal from aqueous solutions of metal-containing dye using pine cone. *Desalin. Water Treat.* **2013**, *51*, 4573–4581. [CrossRef]
15. Thanavel, M.; Kadam, S.K.; Biradar, S.P.; Govindwar, S.P.; Jeon, B.H.; Sadasivam, S.K. Combined biological and advanced oxidation process for decolorization of textile dyes. *SN Appl. Sci.* **2019**, *1*, 1–16. [CrossRef]
16. Bafana, A.; Devi, S.S.; Chakrabarti, T. Azo dyes: Past, present and the future. *Environ. Rev.* **2011**, *19*, 350–371. [CrossRef]
17. Shah, K. Biodegradation of azo dye compounds. *Int. Res. J. Biochem. Biotechnol.* **2014**, *1*, 5–13.
18. Cao, J.; Sanganyado, E.; Liu, W.; Zhang, W.; Liu, Y. Decolorization and detoxification of Direct Blue 2B by indigenous bacterial consortium. *J. Environ. Manag.* **2019**, *242*, 229–237. [CrossRef]
19. Ebrahimi, R.; Maleki, A.; Zandsalimi, Y.; Ghanbari, R.; Shahmoradi, B.; Rezaee, R.; Safari, M.; Joo, S.W.; Daraei, H.; Puttaiah, S.H. Photocatalytic degradation of organic dyes using WO3-doped ZnO nanoparticles fixed on a glass surface in aqueous solution. *J. Ind. Eng. Chem.* **2019**, *73*, 297–305. [CrossRef]
20. Ajaz, M.; Shakeel, S.; Rehman, A. Microbial use for azo dye degradation—A strategy for dye bioremediation. *Int. Microbiol.* **2020**, *23*, 149–159. [CrossRef]
21. Dong, H.; Guo, T.; Zhang, W.; Ying, H.; Wang, P.; Wang, Y.; Chen, Y. Biochemical characterization of a novel azoreductase from *Streptomyces* sp.: Application in eco-friendly decolorization of azo dye wastewater. *Int. J. Biol. Macromol.* **2019**, *140*, 1037–1046. [CrossRef]
22. Ikram, M.; Naeem, M.; Zahoor, M.; Rahim, A.; Hanafiah, M.M.; Oyekanmi, A.A.; Shah, A.B.; Mahnashi, M.H.; Al Ali, A.; Jalal, N.A. Biodegradation of Azo Dye Methyl Red by *Pseudomonas aeruginosa*: Optimization of Process Conditions. *Int. J. Environ. Res. Public Health* **2022**, *19*, 9962. [CrossRef]
23. Selvaraj, V.; Karthika, T.S.; Mansiya, C.; Alagar, M. An over review on recently developed techniques, mechanisms and intermediate involved in the advanced azo dye degradation for industrial applications. *J. Mol. Struct.* **2021**, *1224*, 129195. [CrossRef]
24. Pandey, A.; Singh, P.; Iyengar, L. Bacterial decolorization and degradation of azo dyes. *Int. Biodeterior. Biodegrad.* **2007**, *59*, 73–84. [CrossRef]
25. Chang, J.-S.; Chen, B.-Y.; Lin, Y.S. Stimulation of bacterial decolorization of an azo dye by extracellular metabolites from *Escherichia coli* strain NO_3. *Bioresour. Technol.* **2004**, *91*, 243–248. [CrossRef]
26. Naresh, B.; Jaydip, J.; Prabhat, B.; Rajkumar, P. Recent biological technologies for textile effluent treatment. *Int. Res. J. Biol. Sci* **2013**, *2*, 77–82.

27. Davies, L.C.; Pedro, I.S.; Novais, J.M.; Martins-Dias, S. Aerobic degradation of acid orange 7 in a vertical-flow constructed wetland. *Water Res.* **2006**, *40*, 2055–2063. [CrossRef]
28. Kamika, I.; Momba, M.N.B. Comparing the tolerance limits of selected bacterial and protozoan species to nickel in wastewater systems. *Sci. Total Environ.* **2011**, *410*, 172–181. [CrossRef]
29. Singh, D.; Goswami, R.K.; Agrawal, K.; Chaturvedi, V.; Verma, P. Bio-inspired remediation of wastewater: A contemporary approach for environmental clean-up. *Curr. Res. Green Sustain. Chem.* **2022**, *5*, 100261. [CrossRef]
30. Gomiero, A.; Dagnino, A.; Nasci, C.; Viarengo, A. The use of protozoa in ecotoxicology: Application of multiple endpoint tests of the ciliate *E. crassus* for the evaluation of sediment quality in coastal marine ecosystems. *Sci. Total Environ.* **2013**, *442*, 534–544. [CrossRef]
31. Shakoori, A.R.; Rehman, A. Multiple metal resistance in the ciliate protozoan, *Vorticella microstoma*, isolated from industrial effluents and its potential in bioremediation of toxic wastes. *Bull. Environ. Contam. Toxicol.* **2004**, *72*, 1046–1051. [CrossRef] [PubMed]
32. Sambrook, J.; Fritsch, E.F.; Maniatis, T. *Molecular Cloning: A Laboratory Manual*; Cold Spring Harbor Laboratory Press: New York, NY, USA, 1989; ISBN 0879693096.
33. Regensbogenova, M.; Kisidayova, S.; Michalowski, T.; Javorsky, P.; Moon-Van Der Staay, S.Y.; Moon-Van Der Staay, G.W.M.; Hackstein, J.H.P.; McEwan, N.R.; Jouany, J.P.; Newbold, J.C.; et al. Rapid identification of rumen protozoa by restriction analysis of amplified 18S rRNA gene. *Acta Protozool.* **2004**, *43*, 219–224.
34. Thanavel, M.; Bankole, P.O.; Kadam, S.; Govindwar, S.P.; Sadasivam, S.K. Desulfonation of the textile azo dye Acid Fast Yellow MR by newly isolated *Aeromonas hydrophila* SK16. *Water Resour. Ind.* **2019**, *22*, 100116. [CrossRef]
35. Kalyani, D.C.; Telke, A.A.; Dhanve, R.S.; Jadhav, J.P. Ecofriendly biodegradation and detoxification of Reactive Red 2 textile dye by newly isolated *Pseudomonas* sp. SUK1. *J. Hazard. Mater.* **2009**, *163*, 735–742. [CrossRef] [PubMed]
36. Phugare, S.S.; Kalyani, D.C.; Surwase, S.N.; Jadhav, J.P. Ecofriendly degradation, decolorization and detoxification of textile effluent by a developed bacterial consortium. *Ecotoxicol. Environ. Saf.* **2011**, *74*, 1288–1296. [CrossRef]
37. Bradford, M.M. A Rapid and Sensitive Method for the Quantitation Microgram Quantities of Protein Utilizing the Principle of Protein-Dye Binding. *Anal Biochem.* **1976**, *254*, 248–254. [CrossRef]
38. Israr, M.; Sahi, S.V.; Jain, J. Cadmium accumulation and antioxidative responses in the *Sesbania drummondii* callus. *Arch. Environ. Contam. Toxicol.* **2006**, *50*, 121–127. [CrossRef]
39. Yaseen, D.A.; Scholz, M. Textile dye wastewater characteristics and constituents of synthetic effluents: A critical review. *Int. J. Environ. Sci. Technol.* **2019**, *16*, 1193–1226. [CrossRef]
40. Mani, S.; Chowdhary, P.; Bharagava, R.N. Textile wastewater dyes: Toxicity profile and treatment approaches. In *Emerging and Eco-Friendly Approaches for Waste Management*; Springer: Berlin/Heidelberg, Germany, 2019; pp. 219–244.
41. Jamee, R.; Siddique, R. Biodegradation of synthetic dyes of textile effluent by microorganisms: An environmentally and economically sustainable approach. *Eur. J. Microbiol. Immunol.* **2019**, *9*, 114–118. [CrossRef]
42. Djekoun, M.; Berrebbah, H.; Djebar, M.R. In Vivo Cytotoxicity Assessment of Thiram: Physiological and Biochemical Changes in *Paramecium* sp. *Int. J. Sci. Res. Sci. Eng. Technol.* **2015**, *1*, 320–326.
43. Rehman, A.; Shakoori, F.R.; Shakoori, A.R. Multiple heavy metal tolerant ciliates, *Oxytricha fallax* and *Paramecium caudatum*, isolated from industrial effluents and their potential use in wastewater treatment. *Pak. J. Zool.* **2010**, *42*, 301–309.
44. Ponraj, M.; Gokila, K.; Zambare, V. Bacterial decolorization of textile dye-Orange 3R. *Int. J. Adv. Biotechnol. Res.* **2011**, *2*, 168–177.
45. Maas, R.; Chaudhari, S. Adsorption and biological decolourization of azo dye Reactive Red 2 in semicontinuous anaerobic reactors. *Process Biochem.* **2005**, *40*, 699–705. [CrossRef]
46. Zahid, M.T.; Shakoori, F.R.; Zulfiqar, S.; Al-Ghanim, K.A.; Shakoori, A.R. Growth characteristics, metal uptake and expression analysis of copper metallothionein in a newly reported ciliate, *Tetrahymena farahensis*. *Pak. J. Zool* **2018**, *50*, 1171–1181. [CrossRef]
47. Dopheide, A.; Lear, G.; Stott, R.; Lewis, G. Preferential feeding by the ciliates *Chilodonella* and *Tetrahymena* spp. and effects of these protozoa on bacterial biofilm structure and composition. *Appl. Environ. Microbiol.* **2011**, *77*, 4564–4572. [CrossRef]
48. Khan, Z.; Jain, K.; Soni, A.; Madamwar, D. Microaerophilic degradation of sulphonated azo dye - Reactive Red 195 by bacterial consortium AR1 through co-metabolism. *Int. Biodeterior. Biodegrad.* **2014**, *94*, 167–175. [CrossRef]
49. Amamra, R.; Djebar, M.R.; Grara, N.; Moumeni, O.; Otmani, H.; Alayat, A.; Berrebbah, H. Cypermethrin-induces oxidative stress to the freshwater Ciliate model: *Paramecium tetraurelia*. *Annu. Res. Rev. Biol.* **2015**, 385–399. [CrossRef]
50. Anzenbacher, P.; Anzenbacherova, E. Cytochromes P450 and metabolism of xenobiotics. *Cell. Mol. Life Sci. C.* **2001**, *58*, 737–747. [CrossRef]
51. Benlaifa, M.; Djebar, M.R.; Berredjem, H.; Benamara, M.; Ouali, K.; Djebar, H. Stress induced by cadmium: Its effects on growth respiratory metabolism, antioxidant enzymes and reactive oxygen species (ROS) of *Paramecium* sp. *Int. J. Pharm. Sci. Rev. Res.* **2016**, *38*, 276–281.
52. Benbouzid, H.; Berrebbah, H.; Djebar, M.R. Toxicity of the chlorfenapyr: Growth inhibition and induction of oxidative stress on a freshwater protozoan: *Paramecium* sp. *Adv. Environ. Biol.* **2015**, *9*, 281–285.

53. Giustarini, D.; Colombo, G.; Garavaglia, M.L.; Astori, E.; Portinaro, N.M.; Reggiani, F.; Badalamenti, S.; Aloisi, A.M.; Santucci, A.; Rossi, R. Assessment of glutathione/glutathione disulphide ratio and S-glutathionylated proteins in human blood, solid tissues, and cultured cells. *Free Radic. Biol. Med.* **2017**, *112*, 360–375. [CrossRef] [PubMed]
54. Musaogullari, A.; Chai, Y.-C. Redox regulation by protein S-glutathionylation: From molecular mechanisms to implications in health and disease. *Int. J. Mol. Sci.* **2020**, *21*, 8113. [CrossRef] [PubMed]
55. Bjørklund, G.; Tinkov, A.A.; Hosnedlová, B.; Kizek, R.; Ajsuvakova, O.P.; Chirumbolo, S.; Skalnaya, M.G.; Peana, M.; Dadar, M.; El-Ansary, A. The role of glutathione redox imbalance in autism spectrum disorder: A review. *Free Radic. Biol. Med.* **2020**, *160*, 149–162. [CrossRef] [PubMed]